Supplementary Material (ESI) for Lab on a Chip
This journal is © The Royal Society of Chemistry 2015

Plug-n-play microfluidic systems from flexible assembly of glass-based flow-control modules

Supplementary material

Zhi-Jun Meng,[a] Wei Wang,*[a] Xuan Liang,[a] Wei-Chao Zheng,[a] Nan-Nan Deng,[a] Rui Xie,[a] Xiao-Jie Ju,[a] Zhuang Liu[a] and Liang-Yin Chu*[a,b]

[a] *School of Chemical Engineering, Sichuan University, Chengdu, Sichuan, 610065, China*
E-mail: chuly@scu.edu.cn (L.-Y. Chu), wangwei512@scu.edu.cn (W. Wang); Tel. & Fax: +86 28 8546 0682

[b] *State Key Laboratory of Polymer Materials Engineering, Sichuan University, Chengdu, Sichuan, 610065, China*

Part I. Supplementary STL Files S1-S3.

STL Files S1-S3 for the designs of the support bench (STL S1), positioning groove (STL S2) and connection fastener (STL S3).

Part II. Supplementary Figures S1-S13.

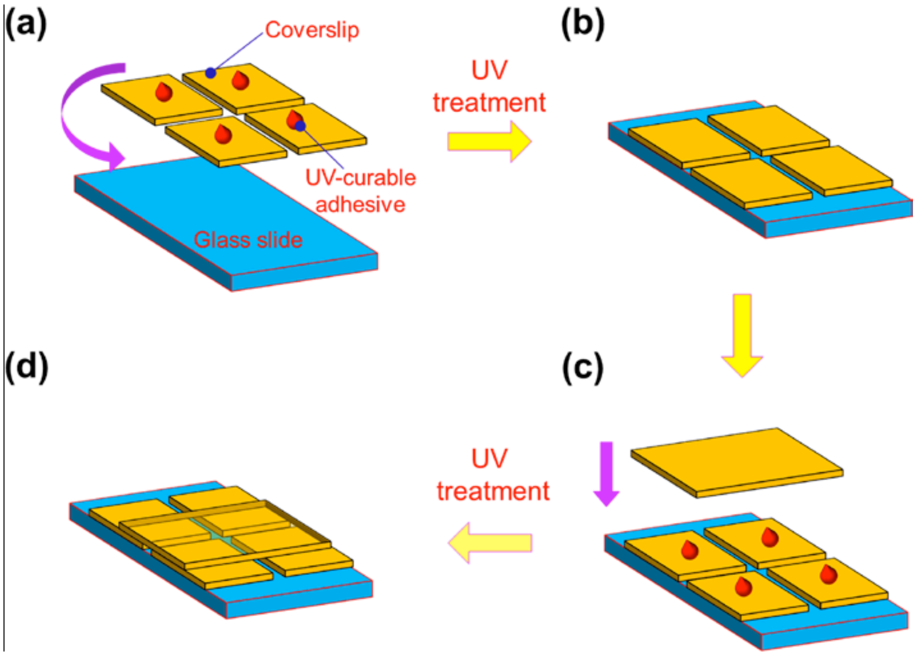

Figure. S1 The patterning process of coverslips and glass slide for fabricating the basic chip. The approach for patterning the well-tailored coverslips on glass slide is based on the strategy that reported by our previous paper (*N. N. Deng, Z. J. Meng, R. Xie, X. J. Ju, C. L. Mou, W. Wang and L. Y. Chu, *Lab Chip*, 2011, **11**, 3963-3969). The coverslips with one side covered with UV-curable adhesive are placed on the glass slide, and then patterned under optical microscope with scales to precisely adjust the microchannel dimension (a). Next, the UV-curable adhesive between the coverslips and the glass slide is solidified under UV light to fix the position of the coverslips (b). After that, the other side of the fixed coverslips are coated with UV-curable adhesive, and then covered with another coverslip (c). Finally, the UV-curable adhesive between the coverslips is solidified under UV light to produce the basic chip (d).

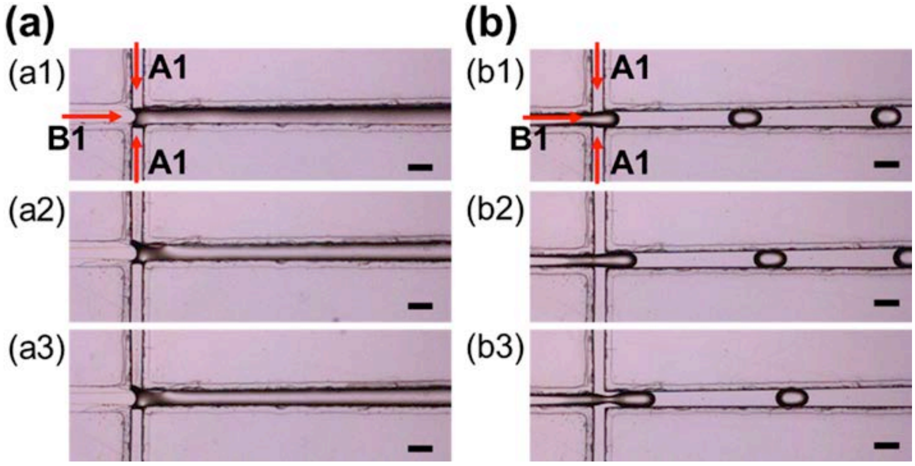

Fig. S2 Optical micrographs of a single flow-control module for generation of O/W emulsions with unmodified glass surface (a) and hydrophilic modified surface (b). (a) Failed generation of O/W emulsions due to the oil wetting on the microchannel wall. (b) Successful generation of O/W emulsions. The solutions are: A1 = DI water + 2 % (w/v) glycerol + 1 % (w/v) F127; B1 = BB:SO (1:1, v/v) + 2 % (w/v) PGPR. The flow rates are: (a) Q_{B1} = 300 μL h^{-1}, and Q_{A1} = 1600 μL h^{-1} (a1), 3000 μL h^{-1} (a2), and 5000 μL h^{-1} (a3); (b) Q_{B1} = 300 μL h^{-1}, and Q_{A1} = 1600 μL h^{-1}. Scale bars are 200 μm.

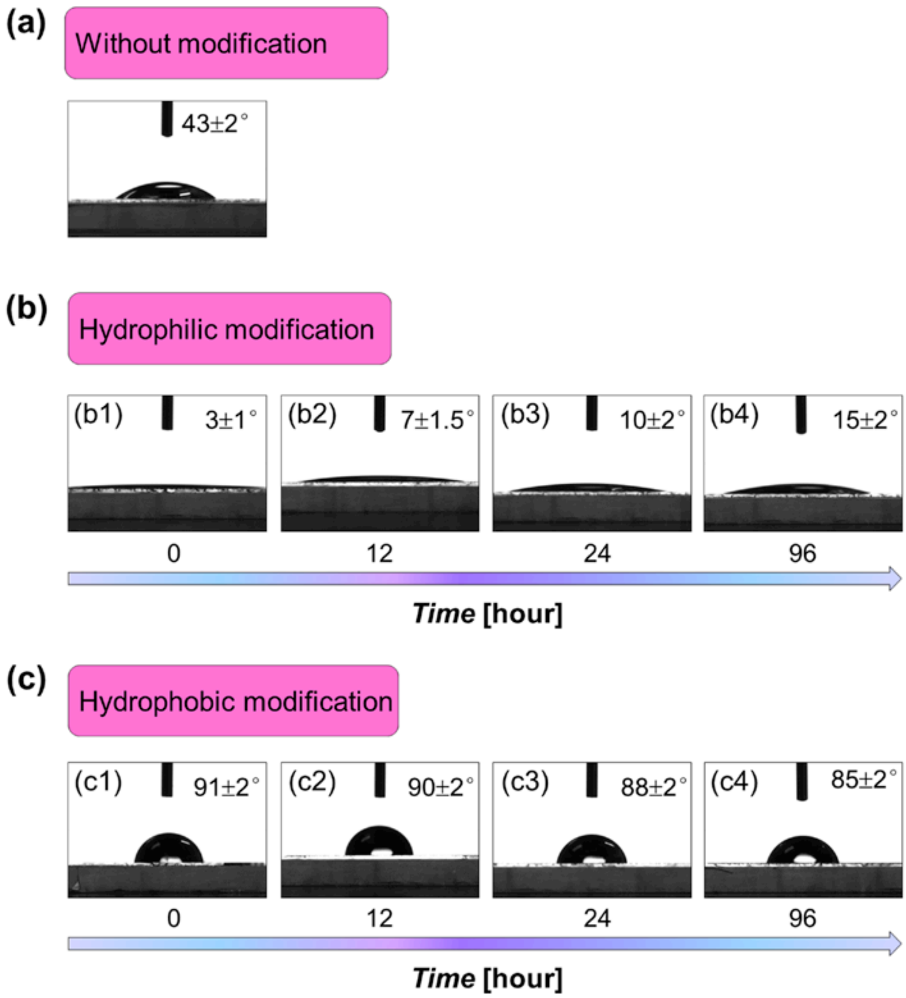

Fig. S3 Time-dependent changes of water contact angles of unmodified (a), hydrophilic modified (b) and hydrophobic modified (c) glass coverslips. First, the coverslips were respectively soaked into the hydrophilic and hydrophobic modification solutions for 20 seconds, and then washed with DI water. Next, the water contact angles were measured by drop shape analyzer (DSA25, KRÜSS GmbH) at 0, 12, 24 and 96 hours after the modification, with unmodified coverslips as the control group. The results show the efficient hydrophilic (b) and hydrophobic (c) modification of the coverslips as compared with the unmodified ones (a). Although the water contact angles of the modified coverslips slightly change after 96 hours, their surface still remains hydrophilic or hydrophobic enough for generating O/W or W/O emulsions. Moreover, the simple modification approach we used in this study also allows easy re-modification of the glass surface.

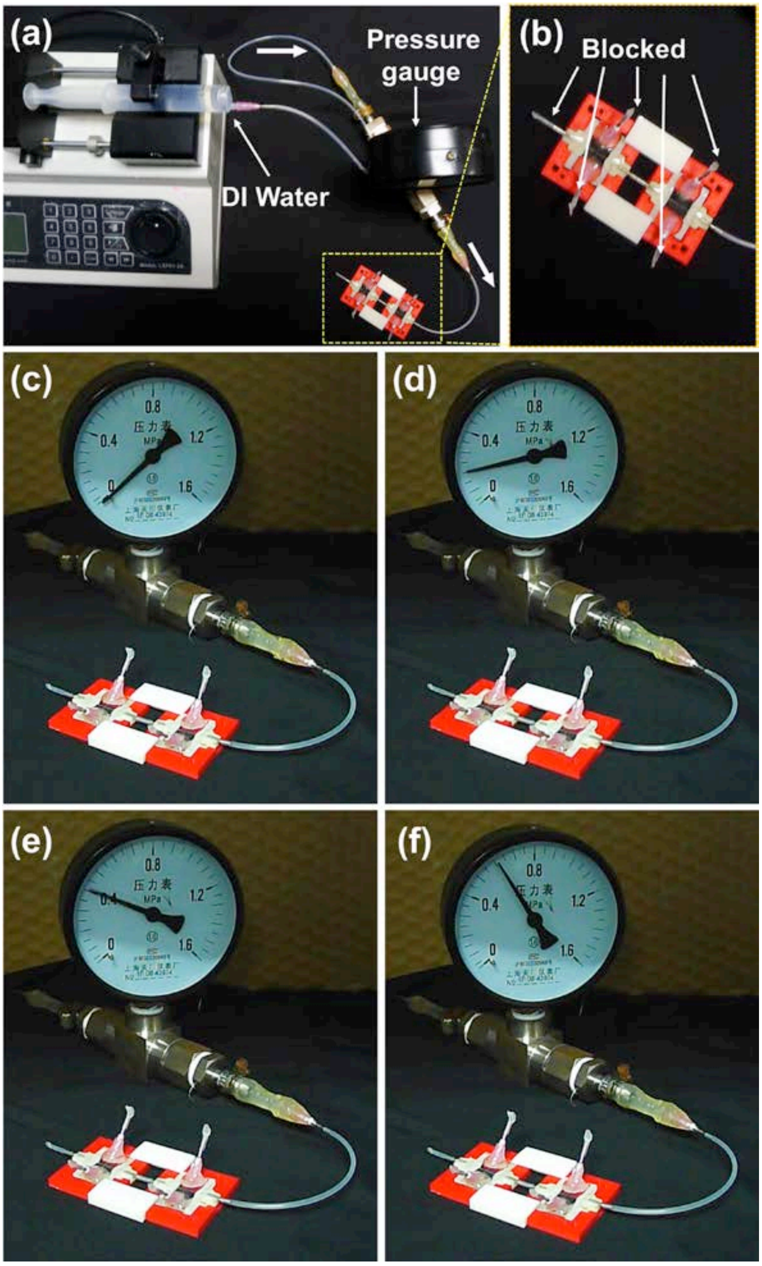

Fig. S4 Photographs showing the pressure test of a two-stage microfluidic system. (a) The two-stage microfluidic system, pressure gauge (Model Y-100, 0~1.6 MPa, Shanghai Tianchuan Meter Instrument Factory), and syringe that mounted on an one-line pump used for setup of the pressure test. (b) The two-stage microfluidic system with only one inlet for injecting fluid for pressure test. (c-f) Pressure tests that showing the intact microfluidic system without any fluid leakage at pressures of 0 (c), 0.2 (d), 0.4 (e) and 0.6 MPa (f).

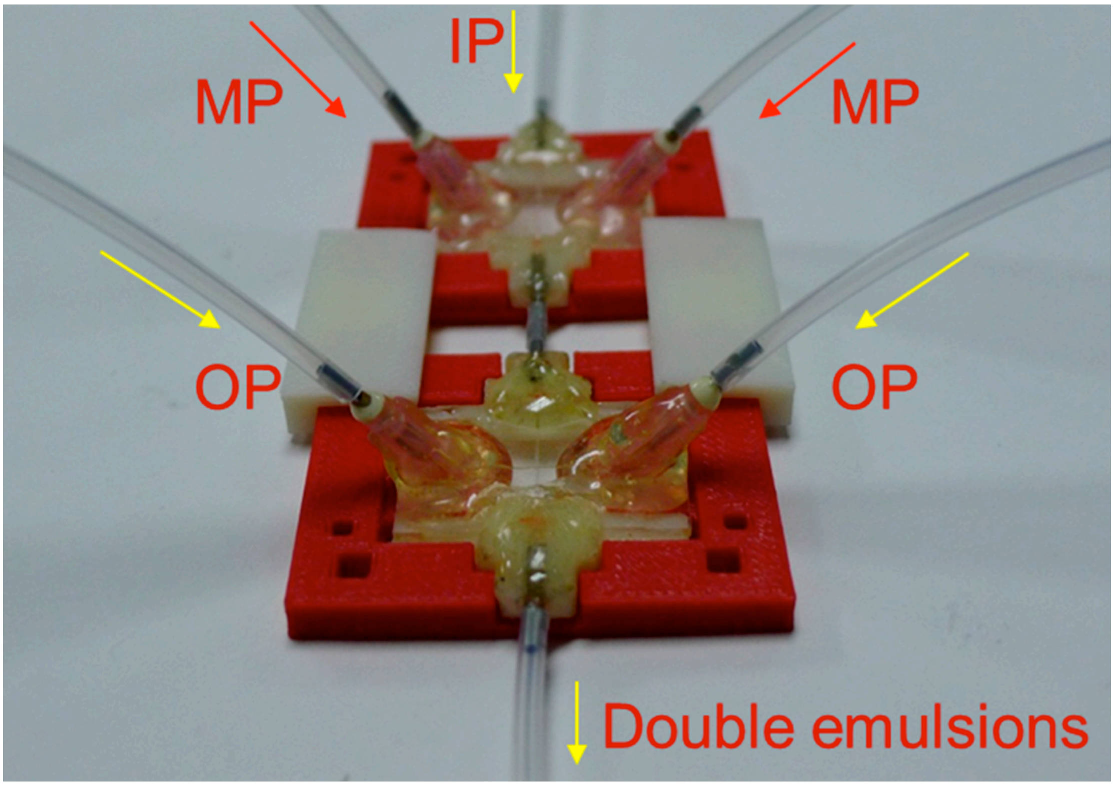

Fig. S5 Photograph showing the connection of PE pipes with the inlet and outlet of a two-stage microfluidic system for injecting inner phase (IP), middle phase (MP), and outer phase (OP) for generating double emulsions.

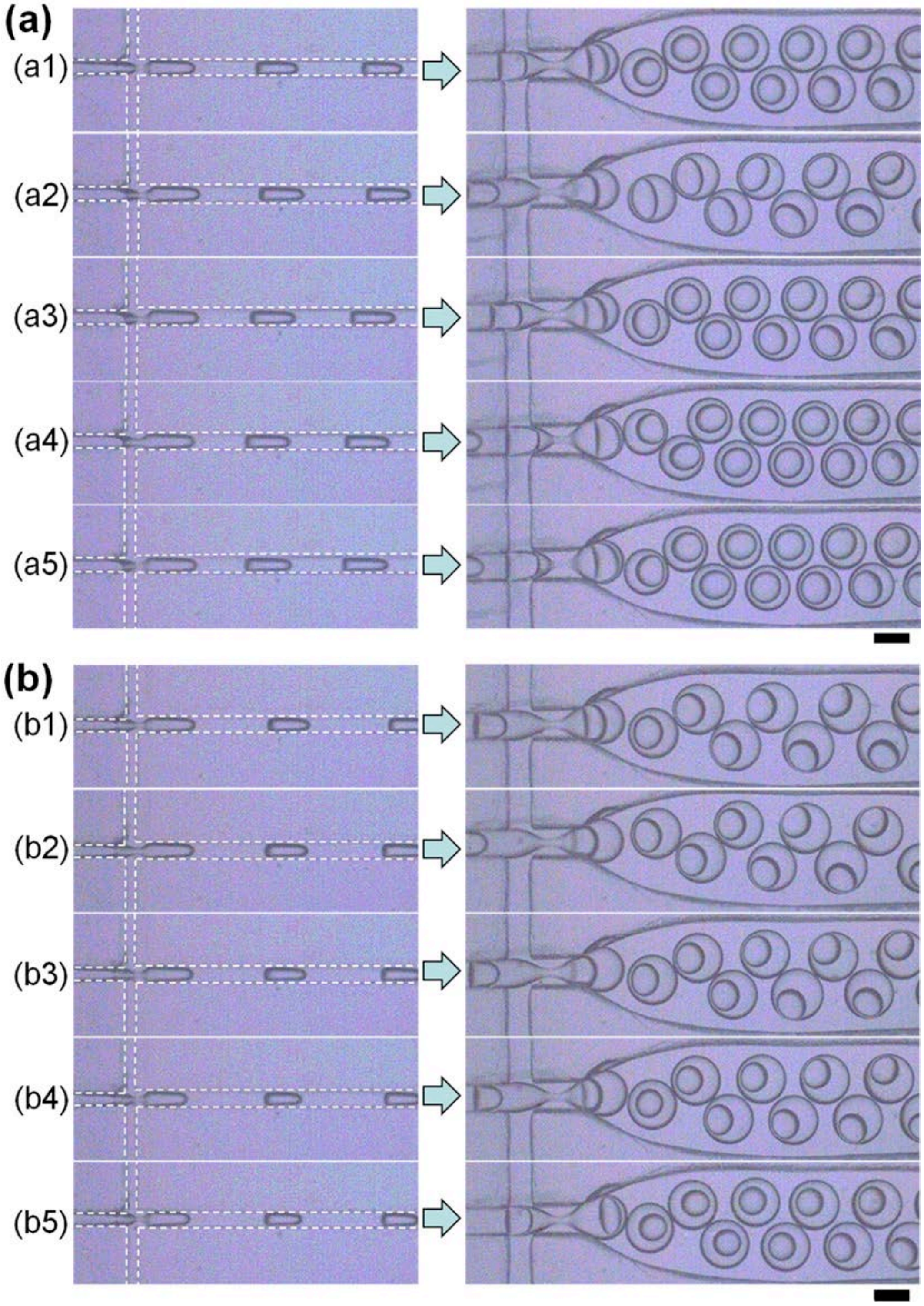

Fig. S6 High-speed video frames of generation of W/O/W double emulsions in a two-stage modular microfluidic system. (a) The flow rates are: Q_{B1} = 800 μL h^{-1}, Q_{A2} = 1600 μL h^{-1}, and Q_{A1} = 250 μL h^{-1} (a1), 275 μL h^{-1} (a2), 300 μL h^{-1} (a3), 325 μL h^{-1} (a4) and 350 μL h^{-1} (a5). (b) The flow rates are: Q_{A1} = 200 μL h^{-1}, Q_{A2} = 1300 μL h^{-1}, and Q_{B2} = 600 μL h^{-1} (b1), 650 μL h^{-1} (b2), 700 μL h^{-1} (b3), 750 μL h^{-1} (b4) and 800 μL h^{-1} (b5). Scale bars are 200 μm.

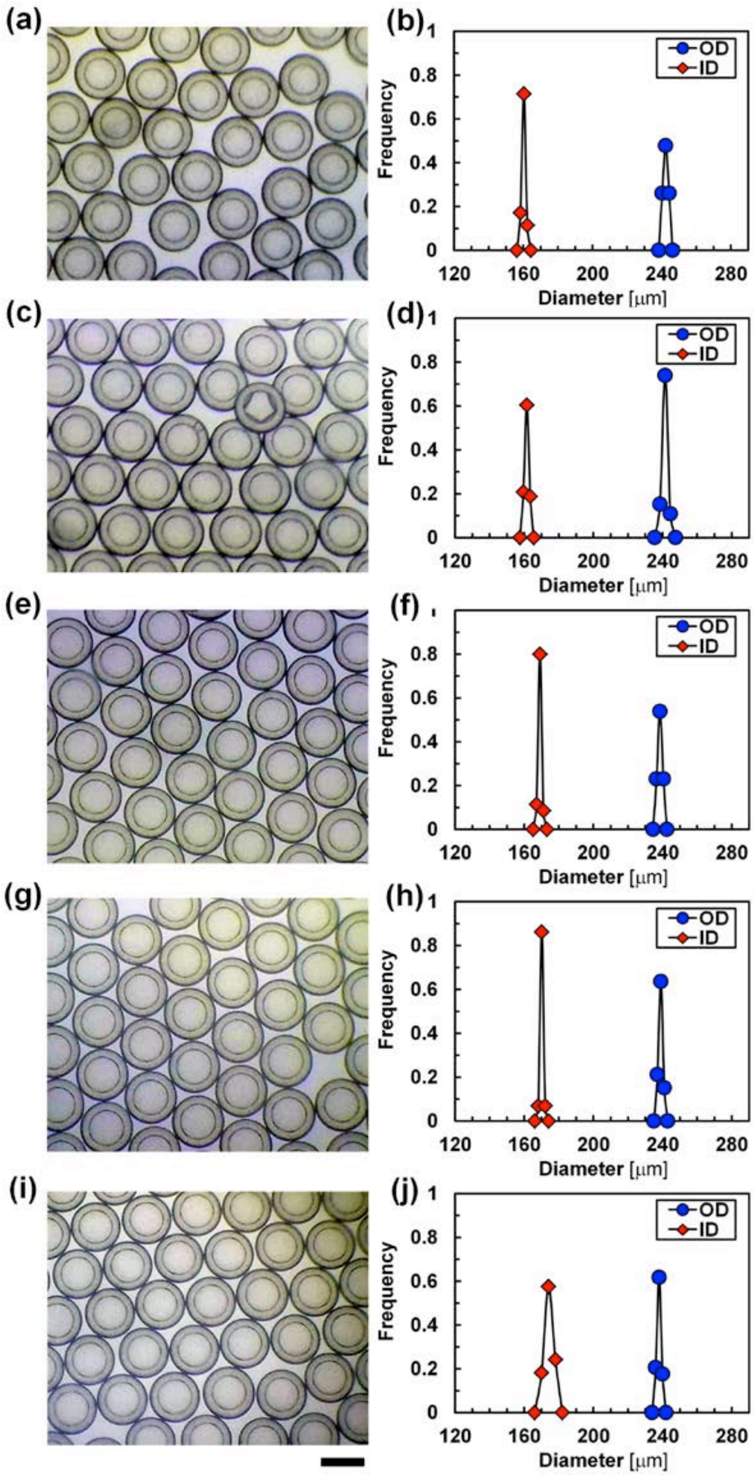

Fig. S7 Optical micrographs (a, c, e, g, i) of the monodisperse W/O/W double emulsions, and the size distribution (b, d, f, h, j) of their inner drop diameter (*ID*) and outer drop diameter (*OD*) as measured from 400 emulsion samples. The flow rates are: Q_{B1} = 800 μL h^{-1}, Q_{A2} = 1600 μL h^{-1}, and Q_{A1} = 250 μL h^{-1} (a), 275 μL h^{-1} (c), 300 μL h^{-1} (e), 325 μL h^{-1} (g) and 350 μL h^{-1} (i). The scale bar is 200 μm.

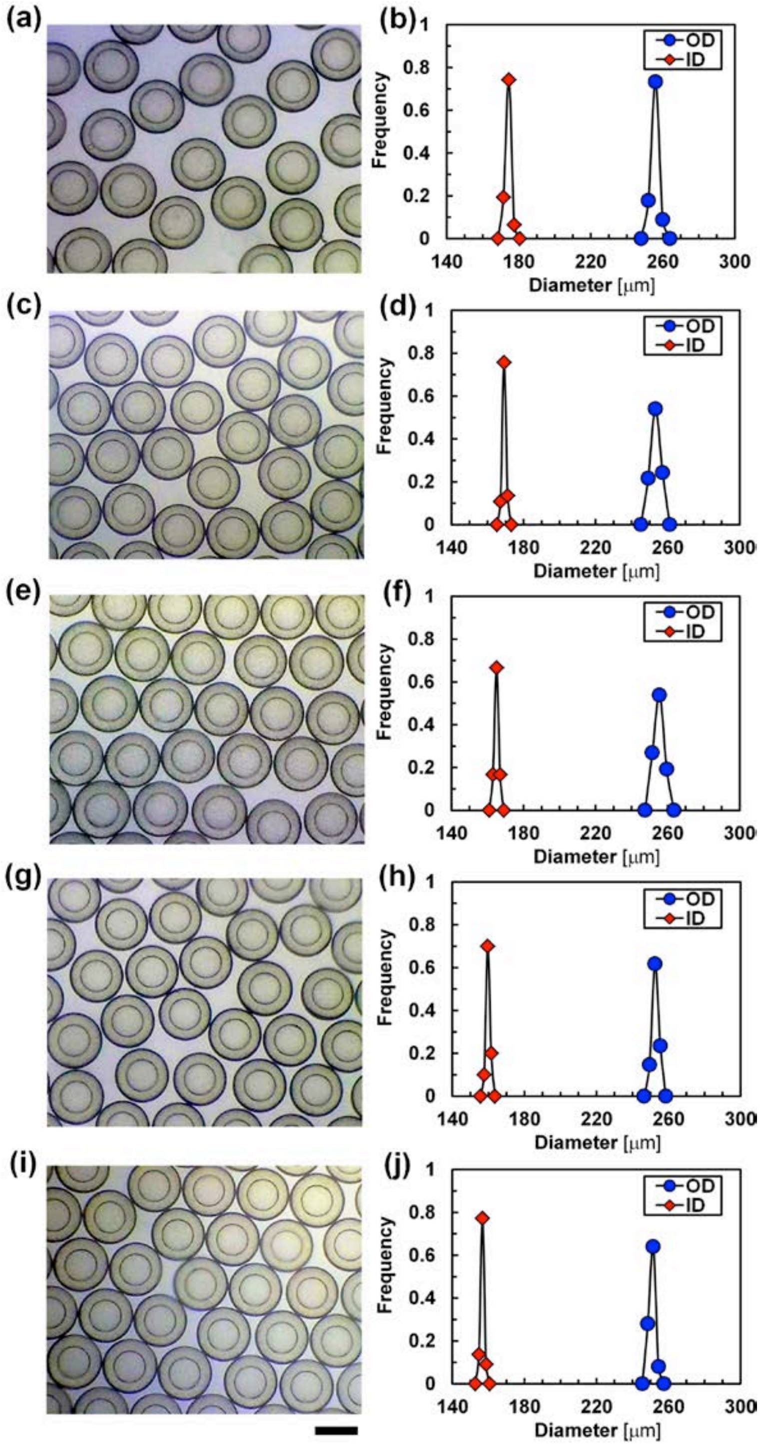

Fig. S8 Optical micrographs (a, c, e, g, i) of the monodisperse W/O/W double emulsions, and the size distribution (b, d, f, h, j) of their inner drop diameter (*ID*) and outer drop diameter (*OD*) as measured from 400 emulsion samples. The flow rates are: Q_{A1} = 200 μL h^{-1}, Q_{A2} = 1300 μL h^{-1}, and Q_{B1} = 600 μL h^{-1} (a), 650 μL h^{-1} (c), 700 μL h^{-1} (e), 750 μL h^{-1} (g) and 800 μL h^{-1} (i). The scale bar is 200 μm.

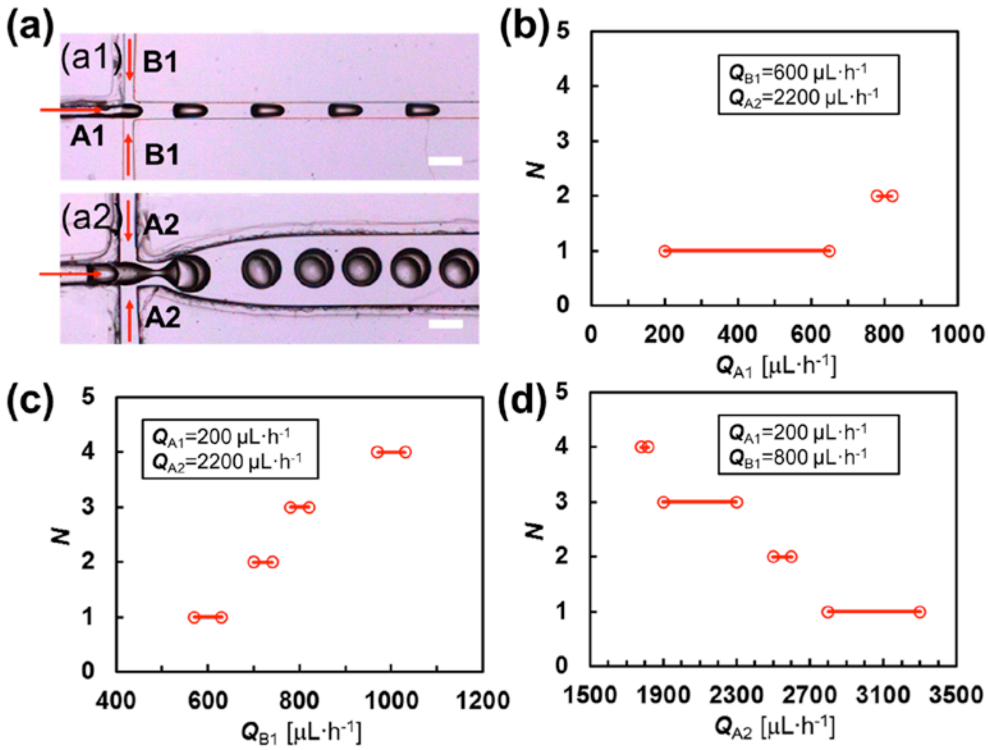

Fig. S9 Effects of flow-rate ranges on the configurations of W/O/W double emulsions generated from a two-stage microfluidic system. (a) High-speed video frames showing the two-step emulsification process for generating W/O/W double emulsions. Scale bars are 200 μm. (b-d) Effects of flow-rate ranges on the numbers of inner drops of W/O/W double emulsions. The flow rates are varied as follows: (b) Q_{A1} is adjusted while Q_{B1} and Q_{A2} are fixed at 600 and 2200 μL h^{-1} respectively; (c) Q_{B1} is adjusted while Q_{A1} and Q_{A2} are fixed at 200 and 2200 μL h^{-1} respectively; (d) Q_{A1} is adjusted while Q_{A1} and Q_{B1} are fixed at 200 and 800 μL h^{-1} respectively.

The results show that the emulsion configurations and flow stabilities are sensitive to the flow rates of each phase. In Fig. S9b, the number of inner drop keeps at one when Q_{A1} ranges from 200 to 600 μL h^{-1}, and keeps at two when Q_{A1} ranges from 780 to 820 μL h^{-1}. In Fig. S9c, the number of inner drop keeps at one, two, three and four when the Q_{B1} ranges are 570~630, 700~740, 780~820 and 970~1030 μL h^{-1} respectively. In Fig. S9d, the number of inner drop keeps at one, two, three and four when the Q_{A2} ranges are 2800~3300, 2500~2600, 1900~2300 and 1780~1820 μL h^{-1} respectively. These results show that the emulsion configurations can be well tuned by adjusting the flow-rate ranges.

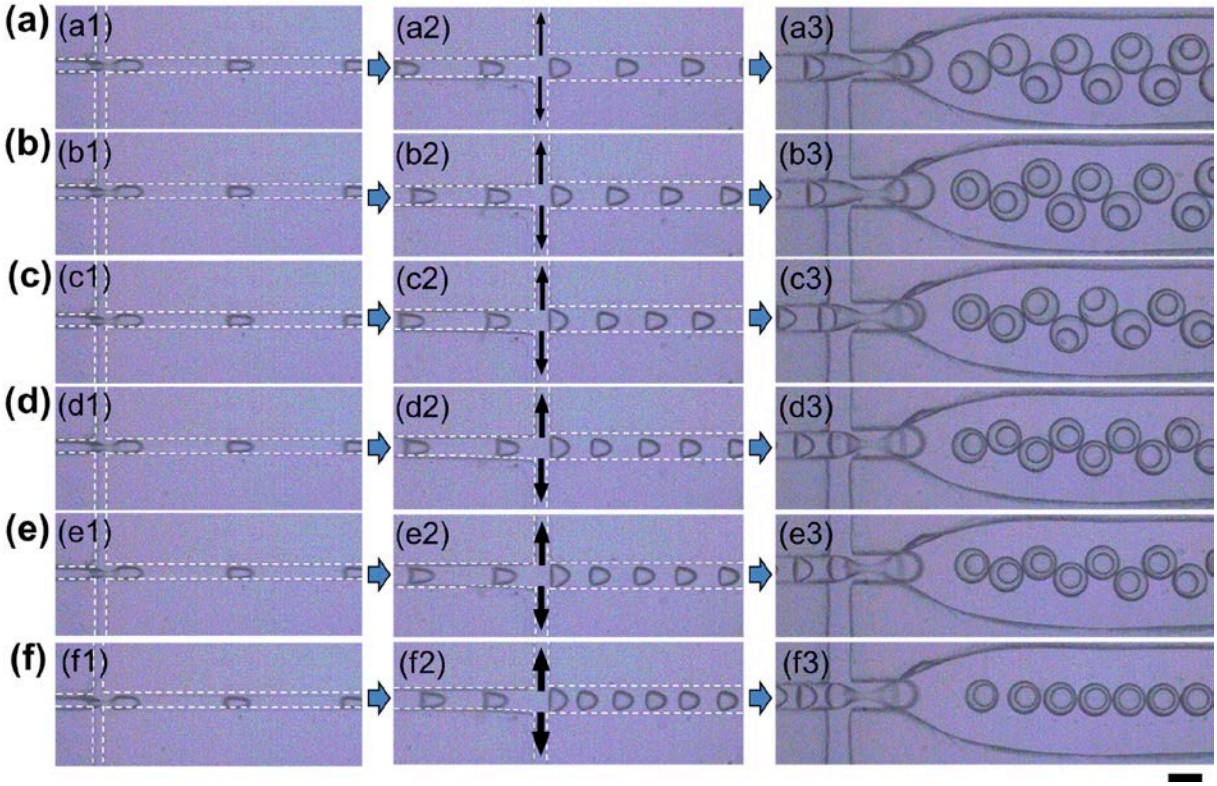

Fig. S10 High-speed video frames of generation of W/O/W double emulsions in a three-stage modular microfluidic system. The flow rates are: Q_{A1} = 200 μL h^{-1}, Q_{B1} = 1400 μL h^{-1}, Q_{A2} = 4000 μL h^{-1}, and $Q_{B1\text{-ex}}$ = 300 μL h^{-1} (a), 400 μL h^{-1} (b), 500 μL h^{-1} (c), 600 μL h^{-1} (d), 700 μL h^{-1} (e), and 800 μL h^{-1} (f). The scale bar is 200 μm.

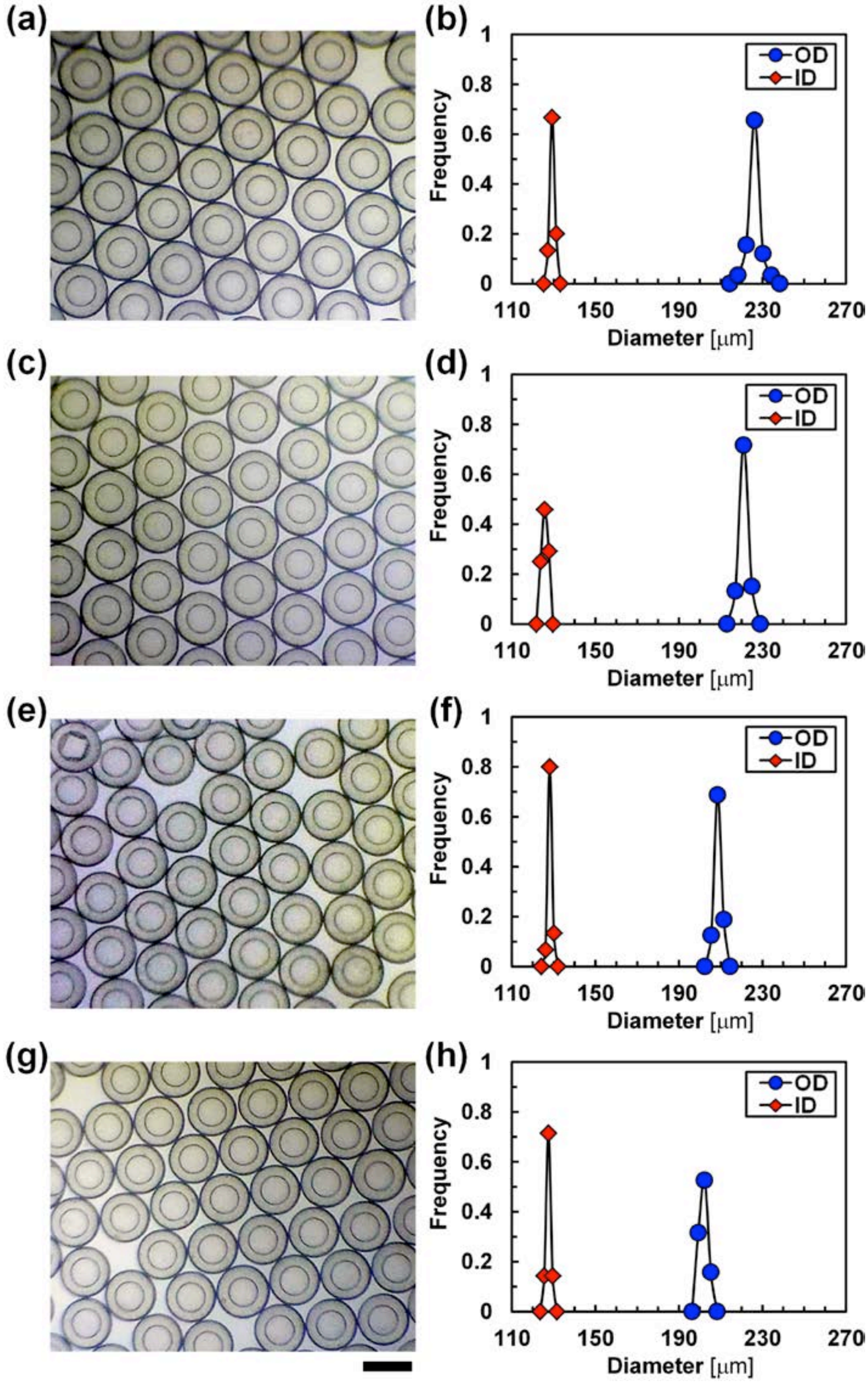

Fig. S11 Optical micrographs (a, c, e, g, i, k) of the monodisperse W/O/W double emulsions, and the size distribution (b, d, f, h, j, l) of their inner drop diameter (*ID*) and outer drop diameter (*OD*) as measured from 400 emulsion samples. The flow rates are: Q_{A1} = 200 μL h^{-1}, Q_{B1} = 1400 μL h^{-1}, Q_{A2} = 4000 μL h^{-1}, and $Q_{B1\text{-}ex}$ = 300 μL h^{-1} (a), 400 μL h^{-1} (c), 500 μL h^{-1} (e), 600 μL h^{-1} (g), 700 μL h^{-1} (i), and 800 μL h^{-1} (k). Scale bar is 200 μm.

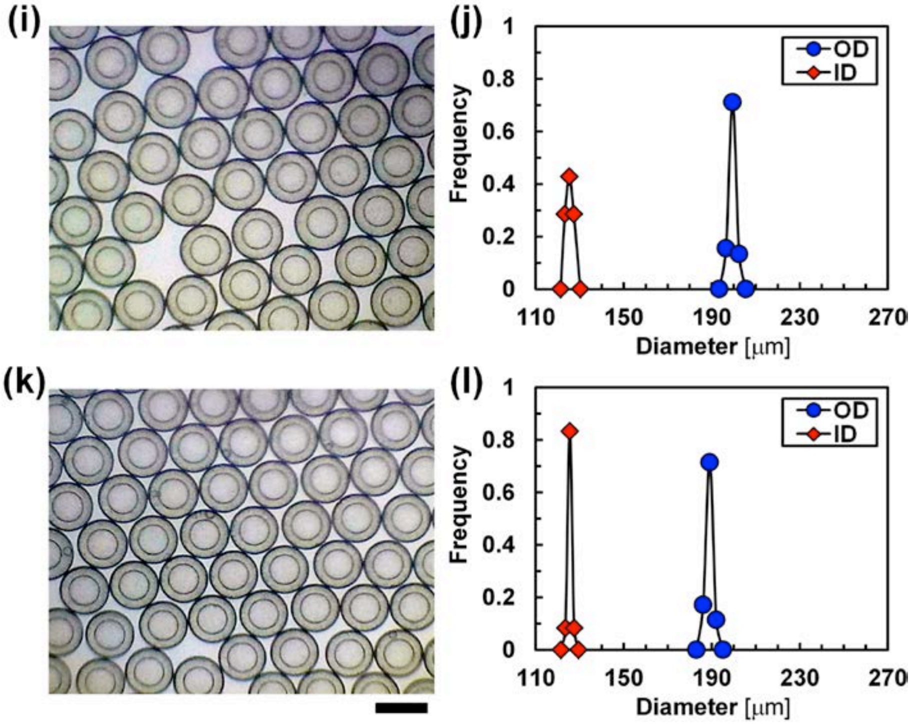

Fig. S11 （*continued*）

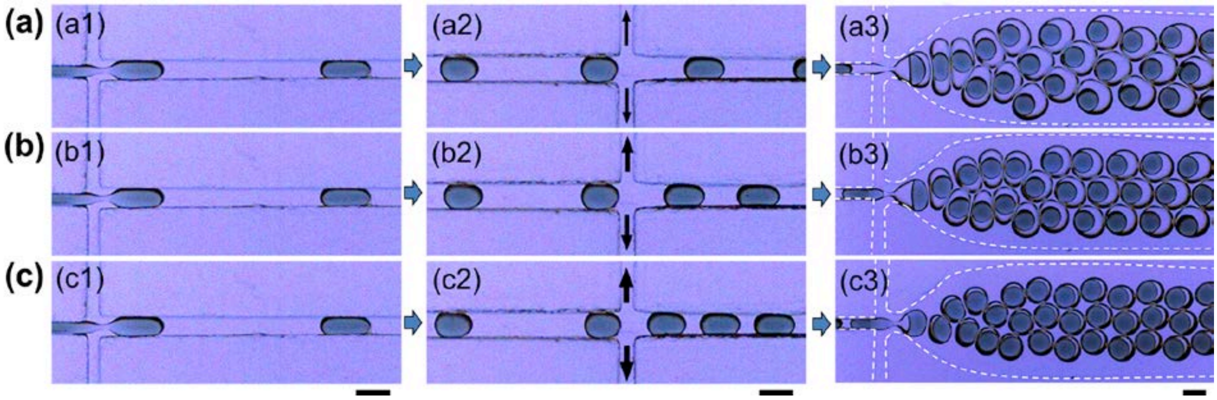

Fig. S12 High-speed video frames of generation of O/W/O double emulsions in a three-stage microfluidic system. The flow rates are: Q_{B2} = 300 μL h^{-1}, Q_{A2} = 1400 μL h^{-1}, Q_{B3} = 600 μL h^{-1}, and $Q_{B2\text{-}ex}$ = 800 μL h^{-1} (a), 1000 μL h^{-1} (b), and 1200 μL h^{-1} (c). Scale bars are 200 μm.

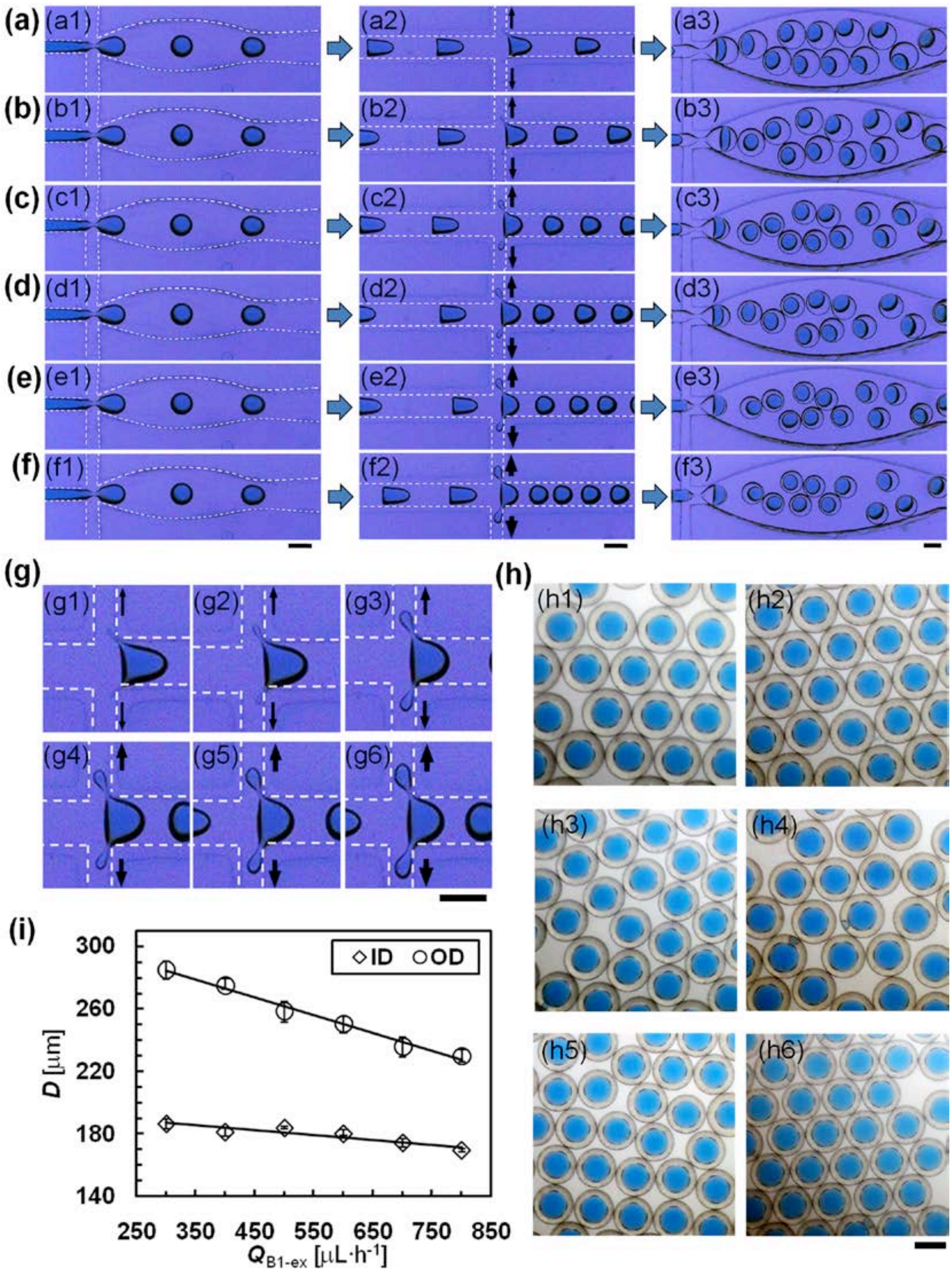

Fig. S13 Passive splitting of dispersed drops at high extracting flow rate of continuous phase. (a-g) High-speed video frames (a-f) of generation of W/O/W double emulsions in a three-stage modular microfluidic system, with magnified frames (g) showing the passive splitting of dispersed water drops (g). (h) Optical micrographs of the obtained monodisperse W/O/W double emulsions. (i) Effect of the extracting flow rate $Q_{B1\text{-ex}}$ on the inner drop diameter (*ID*) and outer drop diameter (*OD*) of the monodisperse W/O/W double emulsions. The flow rates are: Q_{A3} = 200 μL h^{-1}, Q_{B1} = 1000 μL h^{-1}, Q_{A2} = 1600 μL h^{-1}, and $Q_{B1\text{-ex}}$ = 300 μL h^{-1} (a), 400 μL h^{-1} (b), 500 μL h^{-1} (c), 600 μL h^{-1} (d), 700 μL h^{-1} (e), and 800 μL h^{-1} (f). Scale bars are 200 μm.